ACS Medicinal Chemistry Letters

Letter

pubs.acs.org/acsmedchemlett

(7-Benzyloxy-2,3-dihydro-*1H*-pyrrolo[1,2-*a*]indol-1-yl)acetic Acids as $S1P_1$ Functional Antagonists

Daniel J. Buzard,* Luis Lopez, Jeanne Moody, Andrew Kawasaki, Thomas O. Schrader, Michelle Kasem, Ben Johnson, Xiuwen Zhu, Lars Thoresen, Sun Hee Kim, Tawfik Gharbaoui, Dipanjan Sengupta, Lorene Calvano, Ashwin Krishnan, Yinghong Gao, Graeme Semple, Jeff Edwards, Jeremy Barden, Michael Morgan, Khawja Usmani, Chuan Chen, Abu Sadeque, Weichao Chen, Ronald J. Christopher, Jayant Thatte, Lixia Fu, Michelle Solomon, Kevin Whelan, Hussien Al-Shamma, Joel Gatlin, Ibragim Gaidarov, Todd Anthony, Minh Le, David J. Unett, Scott Stirn, Anthony Blackburn, Dominic P. Behan, and Robert M. Jones

Arena Pharmaceuticals, Inc., 6154 Nancy Ridge Drive, San Diego, California 92121, United States

Supporting Information

ABSTRACT: $S1P_1$ is a validated target for treatment of autoimmune disease, and functional antagonists with superior safety and pharmacokinetic properties are being sought as second generation therapeutics. We describe the discovery and optimization of (7-benzyloxy-2,3-dihydro-*1H*-pyrrolo[1,2-*a*]indol-1-yl)acetic acids as potent, centrally available, direct acting $S1P_1$ functional antagonists, with favorable pharmacokinetic and safety properties.

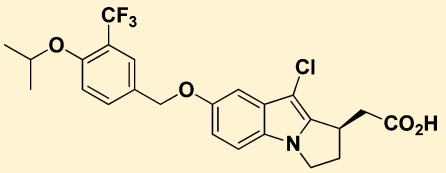

$hS1P_1$ cAMP EC_{50} = 0.021 nM (99%)

KEYWORDS: *Sphingosine-1-phosphate, S1P1 agonist, FTY720, fingolimod, Gilenya*

Sphingosine-1 phosphate (**1**, Figure 1) is a bioactive sphingolipid that binds to the $S1P_{1-5}$ receptors and regulates a variety of cellular functions by signaling through these GPCRs.[1] $S1P_1$ in particular plays an important role in lymphocyte trafficking, and its immunomodulatory function led to the development of Gilenya (**2**, fingolimod) (Figure 1), a nonselective $S1P_1$ agonist currently available in the US for treatment of relapsing forms of multiple sclerosis (MS).[2] *In vivo*, fingolimod is phosphorylated by sphingosine kinase (SPHK2) to (*S*)-monophosphate **3**, which functionally antagonizes $S1P_1$ expressed on T-cells and B-cells through activation (agonism), followed by internalization and proteasomal degradation of the receptor.[3,4] Loss of $S1P_1$ prevents lymphocytes from migrating out of the lymphatic system by interrupting the S1P−$S1P_1$ signaling axis responsible for egress.[5] In MS patients, this results in the sequestration of autoreactive cells in the lymphoid tissues and occluding them from the CNS. Additionally, fingolimod readily crosses the blood−brain barrier and, upon phosphorylation with SPHK2, acts directly on astrocytes via $S1P_1$ to reduce neuroinflammation.[6,7]

Compound **3** is also an agonist of $S1P_3$, $S1P_4$, and $S1P_5$. The $S1P_5$ receptor is present on oligodendrocytes and its activation has been shown to improve barrier integrity and reduce trans endothelial monocyte migration.[8] Notably, several dual $S1P_{1,5}$ agonists are currently being developed as new therapies for MS (e.g., **4**, Figure 1).[9,10] $S1P_4$ is expressed on lymphocytes, hematopoietic cells, and dendritic cells (DCs), and the absence of this receptor decreases T_H17 differentiation of T_H cells.[11] This cell type is associated with MS development, and populations of T_H17 cells in the cerebrospinal fluid of MS patients are generally increased.[12] The majority of medicinal chemistry efforts has focused on identifying $S1P_3$-sparing molecules due to $S1P_3$-dependent bradycardia observed in rodents treated with **2**.[13] Bradycardia is also observed in humans, but it is now thought to arise through activation of $S1P_1$ rather than $S1P_3$,[10,14] which is consistent with the finding that $S1P_3$-sparing agonists have been shown to cause a reduction in heart rate in human trials.[10,15] More recently, $S1P_3$ has been found to be associated with pro-fibrotic properties.[16,17] This may justify continued efforts to avoid interaction with $S1P_3$ in the absence of compelling evidence suggesting a prominent role in disease amelioration.

Fingolimod is associated with a number of other events; such as atrioventricular block, increased blood pressure, macular edema, decreased pulmonary function, respiratory infection, and elevated liver enzymes.[18] Additionally, fingolimod is teratogenic in rodents, and contraception in humans is required during use and for two months following discontinuation of treatment.[18] Presumably the two month period is required due to the relatively long half-life observed in humans (89−157 h). Correspondingly, normalization of lymphocyte levels requires >5 weeks following cessation of fingolimod treatment.[19] A

Received: October 16, 2014
Accepted: November 23, 2014
Published: November 25, 2014

   dx.doi.org/10.1021/ml500422m | *ACS Med. Chem. Lett.* 2014, 5, 1334−1339

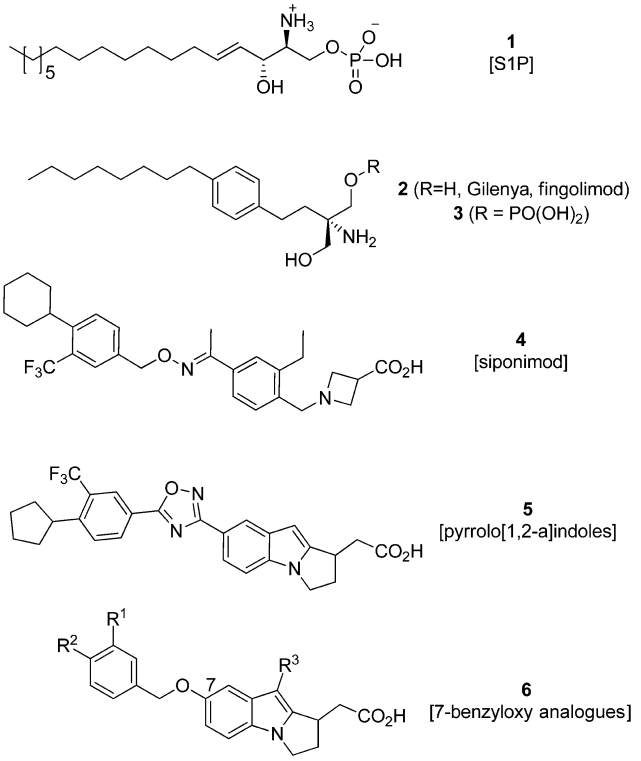

Figure 1. Compounds **1** [Sphingosine-1-phosphate (S1P)], **2** [Gilenya], **3** [Gilenya monophosphate], **4** [siponimod], **5** [pyrrolo-[1,2-*a*]indoles], **6** [7-benzyloxy analogues.

shorter acting agent may be desirable in the event of an opportunistic infection where a rapid return to normal immune functioning would be advantageous.

We, and others, have sought to avoid $S1P_1$ modulators requiring bioactivation (e.g., phosphorylation), instead focusing on carboxylates as phosphate mimetics. Identification of centrally available, nonprodrug modulators has been challenging,[20] and was one factor precluding further development of our earlier series of pyrrolo[1,2a]indoles (e.g., **5**, Figure 1).[21] As an extension of this earlier structure−activity relationship (SAR), we now describe a related series of (7-benzyloxy-2,3-dihydro-1-pyrrolo[1,2-*a*]indol-1-yl)acetic acids (e.g., **6**) as centrally available $S1P_1$ functional antagonists.

Table 1. Racemic 7-Benzyloxy SAR: hS1P$_1$ EC$_{50}$ [cAMP], E_{max}, cLogP, and Lipophilic Efficiency (LiPE)

compd	R^1	R^2	EC_{50} (nM)[a]	E_{max} (%)[b]	cLogP	LiPE
12	CF_3	cyclopentyl	0.095	108	7.13	2.9
13	CN	cyclopentyl	0.49	92	5.82	3.5
14	CF_3	Cl	150	116	5.59	1.2
15	CF_3	CN	83	104	4.51	2.6
16	CN	OCH_3	38	122	3.87	3.6
17	CF_3	OCH_2F	6.7	119	5.41	2.8
18	CF_3	O*i*-Pr	0.15	112	6.07	3.8
19	CN	O*i*-Pr	0.15	105	4.70	5.1
20	CF_3	OCH_2-cyclopropyl	1.1	100	6.21	2.8

[a]EC_{50} values are the mean of three or more replicates. [b]Percent agonism relative to S1P.

Investigation of the (7-benzyloxy-2,3-dihydro-1*H*-pyrrolo-[1,2-*a*]indol-1-yl)acetic acids began with the synthesis of **12**. This analogue was prepared by the synthetic route illustrated in Scheme 1, wherein the key cyclopenta[*a*]indole ring system is constructed in the first step using commercially available indole **7** and butyl acrylate. Subsequent decarboxylation under acidic conditions afforded ketone **8**, which provided a means to introduce the vinyligous *tert*-butyl ester via a Wittig reaction. The hydroxyl group was introduced in two steps by a palladium catalyzed boronic ester synthesis, followed by treatment with hydrogen peroxide. The unsaturated ester was hydrogenated utilizing heterogeneous catalysis to afford intermediate **10**. Etherification with 4-(chloromethyl)-1-cyclopentyl-2-(trifluoromethyl)benzene and removal of the *tert*-butyl ester afforded the desired racemate **12**.

Engagement of $S1P_1$ was evaluated in a homogeneous time-resolved fluorescence (HTRF) cyclase assay, and **12** was found

Scheme 1. (7-Benzyloxy-2,3-dihydro-1-pyrrolo[1,2-*a*]indol-1-yl)acetic Acid Synthesis[a]

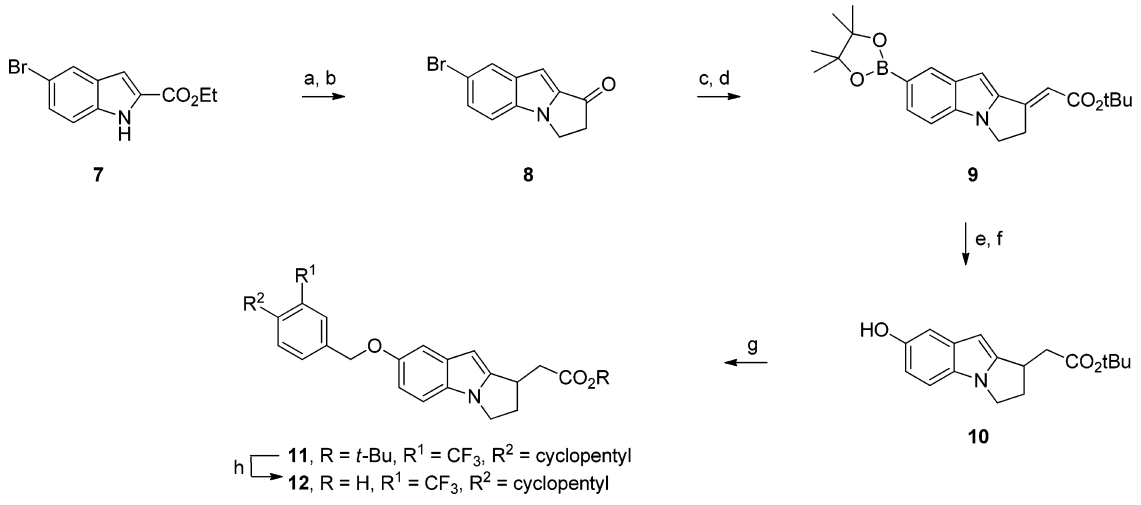

[a]Reagents and conditions: (a) butyl acrylate, NaH, toluene, 110 °C; (b) HCl, AcOH, reflux, 55% (2 steps); (c) (*tert*-butoxycarbonylmethylene) triphenylphosphorane, THF, 65 °C, 72%; (d) pinacol diborane, $PdCl_2$(dppf), dioxane, 90 °C, 100%; (e) hydrogen peroxide, NaOH, THF, rt, 78%; (f) 10% Pd/C, hydrogen (95 psi), EtOAc, rt, 57%; (g) $ArCH_2Cl$, Cs_2CO_3, DMF, 84%; (h) TFA, CH_2Cl_2, room temperature or LiOH, dioxane, 70 °C, 70%.

dx.doi.org/10.1021/ml500422m | *ACS Med. Chem. Lett.* 2014, 5, 1334−1339

Table 2. Human $S1P_{1-5}$ EC_{50} Data

			β-arrestin EC_{50} (nM) (E_{max} %)				
racemate	enantiomers	$S1P_1$ cAMP EC_{50}, (nM) (E_{max} %)	$S1P_1$	$S1P_2$	$S1P_3$	$S1P_4$	$S1P_5$
12	**12a**	0.041 (97)	2.5 (105)	>10000	>10000	570 (47)	107 (83)
	12b	0.32 (100)	20 (100)	>10000	>10000	420 (49)	81 (59)
18	**18a**	0.067 (107)	8.6 (108)	>10000	>10000	>10000	>10000
	18b	0.64 (116)	40 (104)	>10000	>10000	>10000	>10000
19	**19a**	0.13 (98)	11 (128)	>10000	>10,000	>10000	410 (54)
	19b	1.5 (104)	160 (122)	>10000	>10000	>10000	9800 (133)

Table 3. Sprague-Dawley Rat Pharmacokinetics, CNS Distribution, and Lymphocyte Lowering (LL) IC_{50}

enantiomer	Cl_{sys} (L/h/kg)	V_{ss}(L/kg)	C_{max} (μg/mL)	t_{max} (h)	$AUC_{0\text{-}inf}$ (μg·h/mL)	$t_{1/2}$ po (h)	%F	B/P	LL IC_{50} (ng/mL)
12a	0.0721	0.986	0.526	2.67	5.43	9.16	39.0	0.53	24.1
19a	0.131	0.732	0.569	2.00	3.99	3.99	49.8	0.016	210.0

Scheme 2. Stereoselective Synthesis of 24 and 25[a]

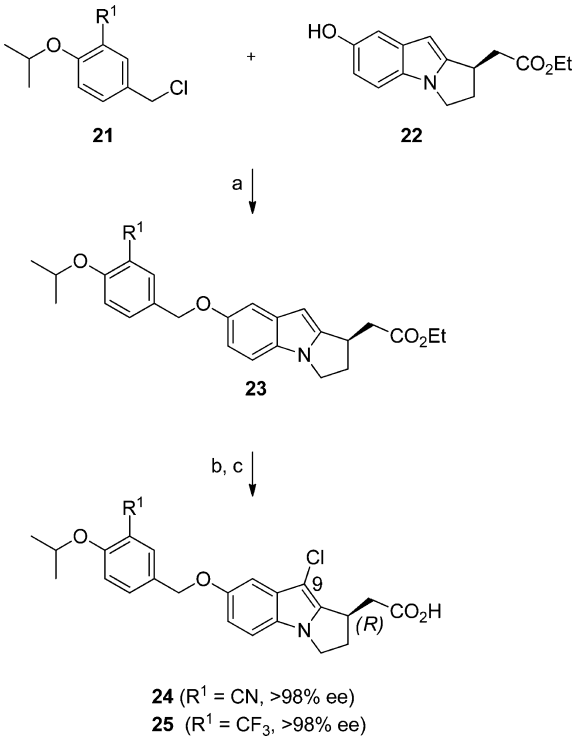

[a]Reagents and conditions: (a) Cs_2CO_3, DMF, rt, 82% (**25**); (b) NCS, CH_2Cl_2, rt, 96% (**25**); (c) NaOH, dioxane, methanol, rt, 94% (**25**).

to be a picomolar agonist (Table 1). Efficacy was measured relative to S1P, and **12** was determined to have an E_{max} value of 108%.

We subsequently examined other 7-benzyloxy groups and screened them in the HTRF assay (Table 1). Lipophilic efficiency (LiPE) values were derived from the functional data point to the 1-isopropoxy-2-(trifluoromethyl)benzene (**18**) and 2-isopropoxy benzonitrile (**19**) as preferable motifs. These racemates, as well as compound **12**, were resolved into their respective enantiomers using chiral chromatography and were evaluated in human $S1P_1$ HTRF, and $S1P_{1-5}$ β-arrestin agonist assays (Table 2). The absolute stereochemistry of each enantiomer tested was not determined at this time. All test compounds were active at $S1P_1$ with one enantiomer in each pair having increased potency relative to the other. A potency shift between HTRF and β-arrestin was observed and is consistent with what we have seen with previous chemical series. Every enantiomer tested was selective against $S1P_2$ and $S1P_3$ with **12a** and **12b** showing appreciable activity at $S1P_4$ and $S1P_5$.

Given the favorable LiPE value of 5.1, **19a** was selected for rat pharmacokinetic and CNS distribution analysis (Table 3). Compound **12a** was also included in this study. A maximal plasma concentration of approximately 500 ng/mL was achieved for both compounds following a 1.0 mg/kg oral dose, and each possessed adequate oral bioavailability (39–49.8%). Compound **12a** exhibited a reduced clearance rate relative to **19a** and had an elimination half-life of 9.16 h, approximately double that of **19a**. Compounds **12a** and **19a** were examined in an abbreviated CNS distribution study wherein brain and plasma drug levels were measured over a 6 h period following a single 1.0 mg/kg oral dose. Interestingly, **19a** showed reduced central exposure relative to **12a** as evidenced by the brain-to-plasma (B/P) ratio (0.016 vs 0.53).

A rat pharmacokinetic/pharmacodynamic (PD/PK) model was utilized to determine the plasma concentration required to reduce lymphocyte counts by 50%. A reduction in circulating lymphocytes is the hallmark property of an $S1P_1$ agonist and is predictive of its immunomodulatory potential. Lymphocyte lowering (LL) IC_{50} determination showed approximately a 10-fold difference in *in vivo* potency between the two analogues (**12a** IC_{50} = 24.1 ng/mL; **19a** IC_{50} = 210 ng/mL). This disparity was also observed *in vitro*, where rat $S1P_1$ EC_{50} values in the β-arrestin platform were 2.5 (**12a**) and 11 nM (**19a**), respectively. In our experience, β-arrestin data has been historically a more reliable predictor of *in vivo* potency than

Table 4. Preclinical Species $S1P_1$ and Human $S1P_{1-5}$ EC_{50} Data

	preclinical species $S1P_1$ EC_{50} cAMP (nM) (E_{max} %)					human $S1P_{1-5}$ EC_{50} β-arrestin (nM) (E_{max} %)				
compd	human	mouse	rat	dog	monkey	$S1P_1$	$S1P_2$	$S1P_3$	$S1P_4$	$S1P_5$
24	0.025 (94)	0.050 (104)	0.072 (93)	0.049 (66)	0.038 (96)	0.63 (112)	>10000	>10000	8600 (85)	47 (84)
25	0.021 (99)	0.064 (95)	0.050 (81)	0.049 (59)	0.058 (84)	0.62 (112)	>10000	>10000	85 (29)	19 (59)

dx.doi.org/10.1021/ml500422m | ACS Med. Chem. Lett. 2014, 5, 1334–1339

Table 5. Sprague-Dawley Rat Pharmacokinetics and Lymphocyte Lowering (LL)

compd	dose iv/po (mg/kg)	Cl_{sys} (L/h/kg)	V_{ss} (L/kg)	C_{max} (μg/mL)	t_{max} (h)	$AUC_{0\text{-}inf}$ (μg·h/mL)	$t_{1/2}$ po (h)	%F	rat LL IC_{50} (ng/mL)
24	1/1	0.192	0.900	0.618	4.00	4.21	3.44	76.4	10.4
25	1/1	0 0926	0 831	0 584	4 67	6 16	5 09	56.6	25.4

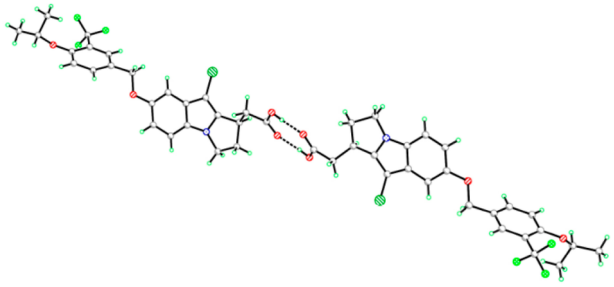

Figure 2. X-ray crystal structure: **25** is triclinic, space group *P*1, with two independent molecules in the asymmetric unit related by a pseudo center of symmetry forming an R22(8) hydrogen bonded dimer.

HTRF, wherein low single digit nanomolar compounds identified in β-arrestin often are quite potent *in vivo*.

Suboptimal *in vivo* potency and limited central exposure prompted further optimization of **19a**. We found the pyrrolo[1,2-*a*]indole ring system amenable to electrophilic substitution in the 9-position, which ultimately led to the identification of **24** and **25** as lead molecules in this chemical series (Scheme 2). A stereoselective synthesis of the (*R*)-ethyl 2-(7-hydroxy-2,3-dihydro-1*H*-pyrrolo[1,2-*a*]indol-1-yl)acetate intermediate **22** was developed[22] and was utilized for preparation of multigram quantities of enantiopure **24** and **25** (Scheme 2). The corresponding *S*-isomers (not depicted) were also evaluated but were significantly less potent.

In vitro, **24** and **25** were evaluated for $S1P_1$ activity in multiple preclinical species and against the five human S1P subtypes (Table 4). Activity was maintained in all species, and neither molecule activated human $S1P_2$ or $S1P_3$. As anticipated, improved β-arrestin potency (**24** IC_{50} = 0.63 nM; **25** IC_{50} = 0.62 nM) translated into robust lymphocyte lowering at relatively low plasma concentration (**24** LL IC_{50} = 10.4 ng/mL; **25** LL IC_{50} = 25.4 ng/mL) (Table 5). Rat PK was similar for both molecules, with **25** possessing a longer elimination half-life (5.09 h vs 3.44 h). Notably, these half-lives are significantly lower than that observed for **12a**. Compound **25** was determined to have a superior brain-to-plasma (B/P) ratio relative to **24** (i.e., 0.27 versus 0.09) in an abbreviated rat CNS distribution study. This may result from the increased lipophilicity of the 1-isopropoxy-2-trifluoromethylbenzene group. Early safety profiling of **24** and **25** revealed no affinity for the hERG channel, and no cardiovascular effects were noted in telemeterized rat. CYP studies showed a weak 2C9 inhibitory potential for **24** (IC_{50} = 8.5 μM), while **25** did not inhibit any of the five major isozymes (>50 μM). Selectivity profiling in a broad panel of receptors and enzymes revealed that **24** possessed moderate affinity for rat P2Y in a [^{35}S]dATPαS competitive binding assay (IC_{50} = 390 nM), but no significant interactions were observed for **25**.

Compound **25** was selected for further preclinical studies including a repeat dose rat CNS distribution study. Rats were dosed with 1.0 mg/kg for six consecutive days and plasma, brain, and cerebrospinal fluid (CSF) samples were taken over a 24 h time period following the last dose. Average plasma and brain concentrations of 352 and 568 ng/mL were achieved and correspond to a *B*/*P* ratio of 1.61. A subsequent rat dose escalation study was performed, and **25** was dose proportional up to 1000 mg/kg po where it reached a maximal concentration (C_{max}) of 72.2 μg/mL.

In addition to rat, a PK/PD analysis was also performed in mouse, and **25** was determined to have an *in vivo* lymphocyte lowering IC_{50} value of 18.3 ng/mL. Given the good lymphocyte lowering achieved in mouse, **25** was subsequently evaluated in a prophylactic experimental autoimmune encephalomyelitis (EAE) model that simulates MS by inducing a demyelinating autoimmune response in female C57Bl/6 mice.[23] Mice were dosed with test compound for 24 days and scoring began on day 10. The following scoring system was utilized: 0 = healthy; 1 = limp tail or hind limb weakness; 2 = limp tail and limb weakness or weakness of 2 or more limbs; 3 = severe limb weakness or single limb paralysis; 4 = paralysis of 2 or more limbs; 5 = death. At a 1.0 mg/kg oral dose, groups treated with either **25** or **2** remained disease free throughout the dosing period (i.e., mean disease score = 0), whereas the vehicle treated group reached a maximal mean disease score of 3.0 at day 20. By day 24, 90% of the animals in the vehicle group had developed disease. At 0.1 and 0.3 mg/kg, **25** exhibited a dose dependent effect on prevention of disease with the 0.3 mg/kg group maintaining a mean disease score of zero at day 24. Minor signs of disease, however, were evident for the 0.1 mg/kg treatment arm (i.e., day 24 mean disease score = 0.7).

The ability of **25** to activate inward-rectifying potassium channels (IKAch) expressed on isolated human atrial myocytes was examined *in vitro*, as this mechanism is believed to be in part responsible for the transient bradycardia observed in humans treated with S1P1 agonists. Both **25** and S1P were tested against this G protein-gated potassium channel and were found to have EC_{50} values of 8.9 and 2.1 nM, respectively. This outcome suggests that **25** may produce a similar reduction in heart rate as has been observed in humans treated with other $S1P_1$ agonists.

Further development of **25** required identification of a suitable solid form for additional preclinical and potential clinical studies. In the course of developing the stereoselective synthesis of **25**, this molecule was observed to form a crystalline, high melting solid (179 °C) upon precipitation in the final step of the synthetic sequence. Larger crystals of the same crystal phase were grown by slow evaporation from acetone and methanol and were suitable for X-ray structure determination. X-ray diffraction revealed a pseudocentrosymmetric hydrogen bonded dimer and confirmed the tentative stereochemical assignment (Figure 2). This crystal phase was found to be poorly soluble in water (<0.001 mg/mL) and prompted a salt screen focused on the conjugate base of the carboxylic acid. Various inorganic and organic counterions were examined before identifying an L-lysine salt of **25** as the preferred development form. The L-lysine adduct is highly crystalline and, unlike the free acid, possesses excellent aqueous solubility (>100 mg/mL). Subsequent physical characterization revealed that the L-lysine salt is anhydrous, nonhygroscopic, and has a high melting onset of 215 °C. Lastly, no thermodynami-

dx.doi.org/10.1021/ml500422m | ACS Med. Chem. Lett. 2014, 5, 1334−1339

cally more stable polymorphs were identified in physical stability testing.

In summary, we have described the discovery and optimization of (7-benzyloxy-2,3-dihydro-1-pyrrolo[1,2-*a*]-indol-1-yl)acetic acids as a new series of selective $S1P_1$ agonists. These agonists were optimized for CNS penetration, *in vivo* potency, and favorable pharmacokinetic and physicochemical properties. Additional information regarding future development of this chemical series will be reported elsewhere.

■ ASSOCIATED CONTENT

Supporting Information

Synthesis and analytical data for compounds **12**−**20**, **24**, and **25**. This material is available free of charge via the Internet at http://pubs.acs.org.

■ AUTHOR INFORMATION

Corresponding Author

*E-mail: dbuzard@arenapharm.com.

Notes

The authors declare no competing financial interest.

■ ABBREVIATIONS

DMF, dimethylformamide; DIAD, diisopropyl azodicarboxylate; THF, tetrahydrofuran; EtOAc, ethyl acetate; hERG, human Ether-à-go-go-Related Gene; CYP, Cytochrome P450; CSF, cerebrospinal fluid; AcOH, acetic acid; CNS, central nervous system; NCS, *N*-chloro succinimide

■ REFERENCES

(1) Brinkmann, V. Sphingosine 1-Phosphate Receptors in Health and Disease: Mechanistic Insights from Gene Deletion Studies and Reverse Pharmacology. *Pharmacol. Ther.* **2007**, *115*, 84−105.

(2) Chun, J.; Brinkman, V. A Mechanistically Novel, First Oral Therapy for Multiple Sclerosis: The Development of Fingolimod (FTY720, Gilenya). *Discovery Med.* **2011**, *12*, 213−228.

(3) Hale, J. J.; Yan, L.; Neway, W. E.; Hajdu, R.; Bergstrom, J. D.; Milligan, J. A.; Shei, G.-J.; Chrebet, G. L.; Thornton, R. A.; Card, D.; Rosenbach, M.; Rosen, H.; Mandala, S. Synthesis, Stereochemical Determination and Biochemical Characterization of the Enantiomeric Phosphate Esters of the Novel Immunosuppressive Agent FTY720. *Bioorg. Med. Chem.* **2004**, *12*, 4803−4807.

(4) Oo, M. L.; Thangada, S.; Wu, M.-T.; Liu, C. H.; Macdonald, T. L.; Lynch, K. R.; Lin, C.-Y.; Hla, T. Immunosuppressive and Anti-angiogenic Sphingosine 1-Phosphate Receptor-1 Agonists Induce Ubiquitinylation and Proteasomal Degradation of the Receptor. *J. Biol. Chem.* **2007**, *282*, 9082−9289.

(5) Matloubian, M.; Lo, C. G.; Cinamon, G.; Lesneski, M. J.; Xu, Y.; Brinkmann, V.; Allende, M. L.; Proia, R. L.; Cyster, J. G. Lymphocyte Egress form Thymus and Peripheral Lymphoic Organs is Dependent on S1P Receptor 1. *Nature* **2004**, *427*, 355−360.

(6) Chun, J.; Hartung, H.-P. Mechanism of Action of Oral Fingolimod (FTY720) in Multiple Sclerosis. *Clin. Neuropharmacol.* **2010**, *33*, 91−101.

(7) Choi, J. W.; Gardell, S. E.; Herrr, D. R.; Rivera, R.; Lee, C.-W.; Noguchi, K.; Teo, S. T.; Yung, Y. C.; Lu, M.; Kennedy, G.; Chun, J. FTY720 (Fingolimod) Efficacy in an Animal Model of Multiple Sclerosis Requires Astrocyte Sphingosine 1-Phosphate Receptor 1 (S1P1) Modulation. *Proc. Natl. Acad. Sci. U.S.A.* **2011**, *108*, 751−756.

(8) van Doorn, R.; Lopes Pinheiro, M. A.; Kooij, G.; Lakeman, K.; von het hof, B.; van der Pol, S.; Geerts, D.; van Horssen, J.; van der Valk, P.; van der Kam, E.; Ronken, E.; Reijerkerk, A.; de Vries, H. E. Sphingosine 1-phosphate Receptor 5 Mediates the Immune Quiescence of the Human Brain Endothelial Barrier. *J. Neuroinflamm.* **2012**, *9*, 133.

(9) Komiya, T.; Sato, K.; Shioya, H.; Inagaki, Y.; Hagiya, H.; Kozaki, R.; Imai, M.; Takada, Y.; Maeda, T.; Kurata, H.; Kurono, M.; Suzuki, R.; Otsuki, K.; Habashita, H.; Nakade, S. Efficacy and Immunomodulatory Actions of ONO-4641, a Novel Selective Agonist for Sphingosine 1-phosphate Receptors 1 and 5, Preclinical Models of Multiple Sclerosis. *Clin. Exp. Immunol.* **2012**, *171*, 54−62.

(10) Gergely, P.; Nusslein-Hildesheim, B.; Guerini, D.; Brinkman, V.; Traebert, M.; Bruns, C.; Pan, S.; Gray, N. S.; Hinterding, K.; Cooke, N. G.; Groenewegen, A.; Vitaliti, A.; Sing, T.; Luttringer, O.; Yang, J.; Gardin, A.; Wang, N.; Crumb, W. J.; Saltzman, M.; Rosenberg, M.; Wallstrom, E. The Selective Sphingosine 1-phosphate Receptor Modulator BAF312 Redirects Lymphocyte Distribution and has Species-specific Effects on Heart Rate. *Br. J. Pharmacol.* **2012**, *167*, 1035−1047.

(11) Schulze, T.; Golfier, S.; Tabeling, C.; Rabel, K.; Graler, M.; Witzenrath, M.; Lipp, M. Sphingosine-1-phosphate Receptor 4 ($S1P_4$) Deficiency Profoundly Affects Dendritic Cell Function and T_H17-cell Differentiation in a Murine Model. *FASEB* **2011**, *25*, 4024−4036.

(12) Jadidi-Niaragh, F.; Mirshafiey, A. The Th17 Cell, the New Player of Neuroinflammatory Process in Multiple Sclerosis. *Scand. J. Immunol.* **2011**, *74*, 1−13.

(13) Forrest, M.; Sun, S.-Y.; Hajdu, R.; Bergstrom, J.; Card, D.; Doherty, G.; Hale, J.; Keohane, C.; Meyers, C.; Milligan, J.; Mills, S.; Nomura, N.; Rosen, H.; Rosenbach, M.; Shei, G.-J.; Singer, I. I.; Tian, M.; West, S.; White, V.; Xie, J.; Proia, R. L.; Mandala, S. Immune Cell Regulation and Cardiovascular Effects of Sphingosine 1-Phosphate Receptor Agonists in Rodents Are Mediated via Distinct Receptor Subtypes. *J. Pharm. Exp. Ther.* **2004**, *309*, 758−768.

(14) Koyrakh, L.; Roman, M. I.; Brinkmann, V.; Wickman, K. The Heart Rate Decrease Caused by Acute FTY720 Administration is Mediated by the G Protein-Gated Potassium Channel I I_{KACh}. *Am. J. Transplant.* **2005**, *5*, 527−536.

(15) Goodman, A. News from the AAN Annual Meeting: Novel Agent Reduces MS. Lesions in Early Trial. *Neurol. Today* **2012**, *12*, 40−42.

(16) Katrin, S.; Menyhart, K.; Killer, N.; Renault, B.; Bauer, Y.; Studer, R.; Steiner, B.; Bolli, M. H.; Nayler, O.; Gatfield, J. Sphinosine 1-Phosphate (S1P) Receptor Agonists Mediate Pro-fibrotic Responses in Normal Human Lung Fibroblasts via S1P2 and S1P3 Receptors and Smad-independent Signaling. *J. Biol. Chem.* **2013**, *288*, 14839−14851.

(17) Takuwa, N.; Okamoto, Y.; Yoshioka, K.; Takuwa, Y. Sphingosine-1-phosphate Signaling and Cardiac Fibrosis. *Inflammation Regener.* **2013**, *33*, 96−108.

(18) Pelletier, D.; Hafler, D. A. Fingolimod for Multiple Sclerosis. *New Engl. J. Med.* **2012**, *366*, 339−347.

(19) Kovarik, J. M.; Schmouder, R.; Barilla, R.; Riviere, G.-J.; Wang, Y.; Hunt, T. Multiple-Dose FTY720: Tolerability, Pharmacokinetics, and Lymphocyte Responses in Healthy Subjects. *J. Clin. Pharmacol.* **2013**, *44*, 532−537.

(20) Demont, E. H.; Arpino, S.; Bit, R. A.; Campbell, C. A.; Deeks, N.; Desai, S.; Dowell, S. J.; Gaskin, P.; Gray, J. R. J.; Harrison, L. A.; Haynes, A.; Heightman, T. D.; Holmes, D. S.; Humphreys, P. G.; Kumar, U.; Morse, M. A.; Osborne, G. J.; Panchal, T.; Philpott, K. L.; Taylor, S.; Watson, R.; Willis, R.; Witherington, J. Discovery of Brain-Penetrant $S1P_3$-Sparing Direct Agonist of the $S1P_1$ and $S1P_5$ Receptors Efficacious at Low Oral Dose. *J. Med. Chem.* **2011**, *54*, 6724−6733.

(21) Buzard, D. J.; Han, S.; Lopez, J.; Kawasaki, A.; Moody, J.; Thoresen, L.; Ullman, B.; Lehmann, J.; Calderon, I.; Zhu, X.; Gharbaoui, T.; Sengupta, D.; Krishnan, A.; Gao, Y.; Edwards, J.; Barden, J.; Morgan, M.; Usmani, K.; Chen, C.; Sadeque, A.; Thatte, J.; Solomon, M.; Fu, L.; Whelan, K.; Liu, L.; Al-Shamma, H.; Gatlin, J.; Le, M.; Xing, C.; Espinola, S.; Jones, R. M. Fused Tricyclic Indoles as S1P1 Agonists with Robust Efficacy in Animal Models of Autoimmune Disease. *Bioorg. Med. Chem. Lett.* **2012**, *22*, 4404−4409.

(22) Schrader, T. O.; Johnson, B. R; Lopez, L.; Kasem, M.; Gharbaoui, T.; Sengupta, D.; Buzard, D.; Basmadjian, C.; Jones, R. M. Complementary Asymmetric Routes to (*R*)-2-(7-Hydroxy-2,3-dihy-

dro-1*H*-pyrrolo[1,2-a]indol-1-yl)acetate. *Org. Lett.* **2012**, *14*, 6306−6309.
(23) Constantinescu, C. S.; Farooqi, N.; O'Brien, K.; Gran, B. Experimental Autoimmune Encephalomyelitis (EAE) as a Model for Multiple Sclerosis (MS). *Br. J. Pharmacol.* **2011**, *164*, 1079−1106.